# JCI-20679 suppresses the proliferation of glioblastoma stem cells by activating AMPK and decreasing NFATc2 expression levels

SHOTA ANDO[1], NAOTO KOJIMA[2], CHIAMI MOYAMA[1], MITSUGU FUJITA[3], KAITO OHTA[2], HIROMI II[1] and SUSUMU NAKATA[1]

Departments of [1]Clinical Oncology and [2]Pharmaceutical Manufacturing Chemistry, Kyoto Pharmaceutical University, Kyoto 607-8414; [3]Center for Medical Education and Clinical Training, Kindai University Faculty of Medicine, Osaka-Sayama, Osaka 589-8511, Japan

Received January 12, 2022; Accepted April 13, 2022

DOI: 10.3892/mmr.2022.12754

**Abstract.** The prognosis of glioblastoma, which is the most frequent type of adult-onset malignant brain tumor, is extremely poor. Therefore, novel therapeutic strategies are needed. Previous studies report that JCI-20679, which is synthesized based on the structure of naturally occurring acetogenin, inhibits mitochondrial complex I and suppresses the growth of various types of cancer cells. However, the efficacy of JCI-20679 on glioblastoma stem cells (GSCs) is unknown. The present study demonstrated that JCI-20679 inhibited the growth of GSCs derived from a transposon system-mediated murine glioblastoma model more efficiently compared with the growth of differentiation-induced adherent cells, as determined by a trypan blue staining dye exclusion test. The inhibition of proliferation was accompanied by the blockade of cell-cycle entry into the S-phase, as assessed by a BrdU incorporation assay. JCI-20679 decreased the mitochondrial membrane potential, suppressed the oxygen consumption rate and increased mitochondrial reactive oxygen species generation, indicating that JCI-20679 inhibited mitochondrial activity. The mitochondrial inhibition was revealed to increase phosphorylated (phospho)-AMPKα levels and decrease nuclear factor of activated T-cells 2 (NFATc2) expression, and was accompanied by a decrease in calcineurin phosphatase activity. Depletion of phospho-AMPKα by knockdown of AMPKβ recovered the JCI-20679-mediated decrease in NFATc2 expression levels, as determined by western blotting and reverse transcription-quantitative PCR analysis. Overexpression of NFATc2 recovered the JCI-20679-mediated suppression of proliferation, as determined by a trypan blue staining dye exclusion test. These results suggest that JCI-20679 inhibited mitochondrial oxidative phosphorylation, which activated AMPK and reduced NFATc2 expression levels. Moreover, systemic administration of JCI-20679 extended the event-free survival rate in a mouse model transplanted with GSCs. Overall, these results suggested that JCI-20679 is a potential novel therapeutic agent against glioblastoma.

## Introduction

Glioblastoma is the most frequent type of adult-onset malignant brain cancer, and the progression of the disease is rapid and aggressive. Multidisciplinary treatments combined with surgical therapy, chemotherapy, and radiation therapy are used for the treatment of glioblastoma; however, the median survival time of patients with glioblastoma is about 15 months. In addition, the 5 years survival rate is less than 10%. Temozolomide is used as standard chemotherapy for glioblastoma treatment, but the prognosis of glioblastoma remains very poor (1,2). A combination of bevacizumab and multidisciplinary treatment is also used, but bevacizumab treatment does not extend overall survival. Therefore, novel therapeutic strategies are needed to improve outcomes in glioblastoma (3).

GSCs are involved in mechanisms of therapy resistance. A cell population in glioblastoma tissue retains characteristics similar to neural stem cells, showing high resistance to treatment (4). This is called the cancer stem-cell hypothesis, and is based on the notion that cell populations that have higher tumorigenicity than surrounding cells are the cause of treatment resistance and the starting point of recurrence (5). Specific inhibition of GSC proliferation is expected to improve the therapeutic outcome of glioblastoma (6).

In recent years, the importance of mitochondria in the pathogenesis of cancer has been realized (7). Metformin, which is a mitochondrial complex I inhibitor, reduces the resistance of glioblastoma to temozolomide (8). In addition, enhanced mitochondrial functions are involved in the resistance of glioblastoma to radiation therapy (9). Therefore,

*Correspondence to:* Dr Susumu Nakata, Department of Clinical Oncology, Kyoto Pharmaceutical University, 5, Misasagi-Nakauchi-cho, Yamashina-ku, Kyoto 607-8414, Japan
E-mail: snakata@mb.kyoto-phu.ac.jp

*Abbreviations:* GSCs, glioblastoma stem cells; DMSO, dimethyl sulfoxide; NFATc2, nuclear factor of activated T-cells 2; ROS, reactive oxygen species; CAMKII, $Ca^{2+}$/calmodulin-dependent protein kinase II; CCCP, carbonyl cyanide m-chlorophenylhydrazone

*Key words:* JCI-20679, glioblastoma, glioblastoma stem-cell, mitochondria, AMPK, nuclear factor of activated T-cells 2

inhibiting mitochondrial functions may be a new therapeutic strategy for glioblastoma treatment.

The synthesis of JCI-20679 was based on the structure of solamin (10), which is a naturally occurring acetogenin analogue contained in plants of the *Annonaceae* family. JCI-20679 inhibits the proliferation of various types of cancer cells (11-14). Upon treatment, JCI-20679 localizes in the mitochondria and shows anti-proliferative effects on the human lung cancer cell line NCI-H23. JCI-20679 also shows anticancer effects without evidence of serious side effects in a mouse model that uses transplantation of NCI-H23 cells (15).

In this study, we hypothesized that JCI-20679 would be an effective therapeutic strategy for glioblastoma. We evaluated the effects of JCI-20679 in primary GSCs models and investigated its mechanisms of action.

## Materials and methods

*Reagents*. JCI-20679 was synthesized as described previously (11) and dissolved in dimethyl sulfoxide (DMSO; 13445-45, Nacalai Tesque, Kyoto, Japan). Compound C (044-33751, Wako Pure Chemical Industries, Osaka, Japan), inosine (I4125, Sigma-Aldrich, St. Louis, MO, USA), CCCP (M34152, Thermo Fisher Scientific, Waltham, MN, USA), rotenone (R8875, Sigma-Aldrich) and cyclosporin A (031-24931, Wako Pure Chemical Industries) were dissolved in DMSO.

*Animals*. Wild-type C57BL/6 and BALB/c mice were obtained from Oriental BioService (Kyoto, Japan). The mice were handled in the animal facility of the Bioscience Research Center at Kyoto Pharmaceutical University according to a protocol approved by the Institution Animal Care and Use Committee.

*Glioblastoma induction*. The procedure was performed as described previously (16,17). Briefly, to generate *Sleeping-Beauty* transposon-mediated *de novo* glioblastoma, neonatal mice under hypothermia anesthesia were placed in a stereotaxic instrument (51730D, Stoelting Co., Wood Dale, IL, USA). DNA complexed with polyethyleneimine was injected into the lateral cerebral ventricle at 1 $\mu$l/min for 2 min using a 10 $\mu$l Hamilton syringe with a 30 gauges needle and an automated infusion system (Legato 130, KD Scientific, Holliston, MA, USA). The coordinates for DNA injection were +1.5 AP, 0.7 ML, and -1.5 DV from λ. In vivo-JetPEI (101000040, Polyplus Transfection, New York, NY, USA), which is an *in vivo*-compatible DNA transfection reagent, was used. The following DNA plasmids were used for glioblastoma induction: PT2/C-Luc//PGK-SB13 (0.2 $\mu$g, 20207, Addgene, Watertown, MA, USA), PT/Caggs-NRASV12 (0.4 $\mu$g, 20205, Addgene), PT3.5/CMV-EGFRvIII (0.4 $\mu$g, 20280, Addgene), and PT2-shP53 (0.4 $\mu$g, 124261, Addgene). Tumor formation was confirmed 10 min after injection of D-luciferin (126-05116, Wako) into the abdominal cavity of the 1-3 months old mice using an IVIS Lumina XR imaging system (Summit Pharmaceuticals International, Tokyo, Japan). Mice were sacrificed by using cervical dislocation for glioblastoma tissue collection.

*Cell culture*. The procedure used to establish primary GSCs was performed as described previously (17). Briefly, tumor tissues were diced with scalpels and digested with accutase (AT-104, Innovative Cell Technologies, San Diego, CA, USA) at 37˚C for 20-30 min, and then washed and incubated with serum-free neural stem-cell culture medium consisting of neurobasal medium supplemented with B27, N2 (17504044, 17502001, Gibco/Thermo Fisher Scientific), and 10 ng/ml EGF and bFGF (236-EG-200, 233-FB-025, R&D Systems, Minneapolis, MN, USA) to maintain GSCs as neurospheres. The neurospheres were split into single cells using accutase and maintained in neural stem-cell culture medium. The procedure to establish differentiated glioblastoma cell lines in an adherent culture system was performed as described previously (18). A172 and U251 human adherent glioblastoma cells obtained from Riken BRC (Tsukuba, Japan) were maintained in DMEM supplemented with 10% FBS (175012, HyClone, South Logan, UT, USA) and penicillin-streptomycin (15140-148, Gibco/Thermo Fisher Scientific). All cells were incubated at 37˚C in a 5% $CO_2$ atmosphere.

*BrdU incorporation assay*. GSCs were treated with JCI-20679 at the indicated concentrations for 72 h. The cells were harvested, and the proportion of cells in the DNA synthesis phase was detected by using an APC BrdU flow kit (552598, BD Biosciences, San Diego, CA, USA) following the manufacturer's instructions. At least 3,000 cells per specimen were measured and assessed by flow cytometry using a BD LSRFortessa X-20 cell analyzer (BD Biosciences).

*Measurement of mitochondrial membrane potential*. Mitochondrial membrane potentials were detected using JC-1 MitoMP Detection kit (MT09, Dojindo Laboratories, Kumamoto, Japan) according to the manufacturer's instructions and assessed by flow cytometry using a BD LSRFortessa X-20 cell analyzer (BD Biosciences). For monitoring the mitochondrial membrane potential, we used the PE and FITC fluorescence as the JC-1 red and JC-1 green fluorescence. The mitochondrial membrane potential was analyzed by using the ratio of the mean of the JC-1 red/green fluorescence signal intensities.

*Measurement of oxygen consumption rate*. The oxygen consumption rate was measured using an extracellular oxygen consumption assay (ab197243, Abcam, Cambridge, UK) according to the manufacturer's instructions. At least 700,000 cells per specimen were analyzed every minute for 1 h. These data were normalized by cell numbers.

*Measurement of mitochondrial ROS*. Mitochondrial reactive oxygen species (ROS) were measured using MitoRos 580 dye optimized for detecting ROS in mitochondria (16052, AAT Bioquest, Sunnyvale, CA, USA) according to the manufacturer's instructions, and were assessed by flow cytometry using a BD LSRFortessa X-20 cell analyzer (BD Biosciences). At least 10,000 cells per specimen were measured.

*Measurement of the AMP/ATP ratio*. The procedure was carried out as described previously (19). Briefly, cellular ATP was measured using a CellTiter-Glo luminescent cell viability assay kit, and cellular AMP was measured using an AMP-Glo assay kit (G7570, V5011, Promega, Madison, WI, USA), and then the AMP/ATP ratio was calculated.

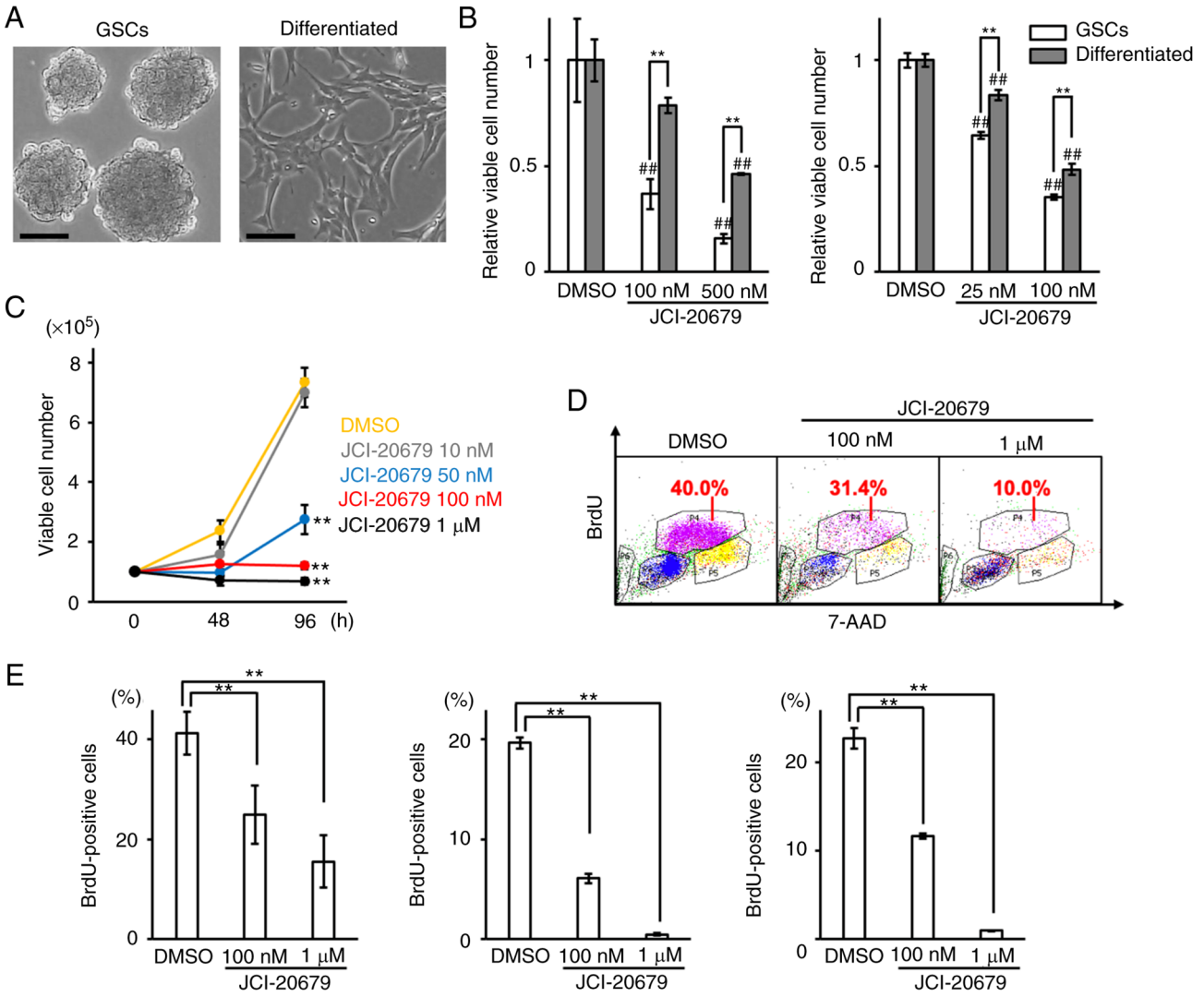


Figure 1. JCI-20679 suppresses the proliferation of glioblastoma stem cells. (A) Representative images of GSCs maintained as neurospheres and differentiation-induced cells maintained in adherent culture (scale bar, 100 $\mu$m). (B) Relative number of viable GSCs and differentiated glioblastoma cells after treatment with JCI-20679 for 72 h in two independent lines of GSCs (GSCs in the left panel, n=4; GSCs in the right panel and differentiated glioblastoma cells in the both panels, n=3). The number of viable cells was counted using trypan blue staining. The number of viable cells was normalized with the results of each DMSO-treated control. $^{**}$P<0.01 as indicated; $^{\#\#}$P<0.01 vs. DMSO by 2-way ANOVA with Bonferroni's multiple comparison test. (C) Number of viable GSCs after treatment with JCI-20679 at the indicated concentrations (n=4). The number of viable cells was counted by trypan blue staining. $^{**}$P<0.01 by one-way ANOVA with Dunnett's multiple comparisons test. (D) Percentage of cells in the DNA synthesis phase as evaluated by BrdU incorporation. The proportions of BrdU-positive S-phase cells were described. (E) Quantitative analysis of the proportion of BrdU-positive S-phase cells in three different GSC lines (n=3, respectively). $^{**}$P<0.01 by one-way ANOVA with Dunnett's multiple comparisons test. All data are presented as mean ± SD. GSCs, glioblastoma stem-cells; DMSO, dimethyl sulfoxide.

*Knockdown of AMPKβ*. The procedure was performed as described previously (17). Briefly, RNAi clones targeting AMPKβ were obtained from Sigma-Aldrich. Transduction using lentiviruses with non-targeting shRNA (SHC016, Sigma-Aldrich, Sequence: CCGGGCGCGATAGCGCTAATAATT TCTCGAGAAATTATTAGCGCTATCGCGCTTTTT) or shRNA targeting AMPKβ was performed at a multiplicity of infection of 10. The following shRNAs were used: sh-AMPKβ #1 (TRCN0000025105, Sequence: CCGGCCCTCCTCTAC AAGCCGATATCTCGAGATATCGGCTTGTAGAGGAGG GTTTTT), sh-AMPKβ #2 (TRCN0000274638, Sequence: CCGGCCATGATCCTTCTGAGCCAATCTCGAGATTGG CTCAGAAGGATCATGGTTTTT). The cells were maintained with 0.75 $\mu$g/ml puromycin (164-23154, Wako Pure Chemical Industries).

*Western blot analysis*. To extract proteins, cells were lysed by 1% SDS buffer supplemented with a protease inhibitor cocktail for use with Mammalian Cell and Tissue Extracts (25955-11, Nacalai Tesque) and PhosSTOP EASYpack (04 906 845 001, Roche Diagnostics, Indianapolis, IN, USA). Total proteins were separated by SDS-PAGE and transferred to PVDF membranes (IPVH00010, Millipore, Billerica, MA, USA). The membranes were blocked with 3-5% fat-free dried milk or 5% BSA in Tris-buffered saline (TBS; 50 mM Tris, 2.68 mM KCl, 137 mM NaCl, PH 7.4) with 0.05% Tween20 (TBST) or Blocking One-P (05999-84, Nacalai Tesque), and then incubated with primary and secondary antibodies. The chemiluminescence of proteins was detected using a ChemiDoc XRS Plus system (Bio-Rad) through the reaction with Clarity Western ECL substrate (170-5060, Bio-Rad

Laboratories, Hercules, CA, USA) or ChemiLumi One Super substrate (02230-30, Nacalai Tesque). The following antibodies were used; p-AMPKα (1:1,000; 2535, Cell Signaling Technology, Danvers, MA, USA), AMPKα (1:1,000; 5832, Cell Signaling Technology), GAPDH (1:1,000; 016-25523, Wako Pure Chemical Industries), p-CAMKII (1:1,000; 12716, Cell Signaling Technology), CAMKII (1:1,000; 4436, Cell Signaling Technology), NFATc2 (1:1,000; 5861, Cell Signaling Technology), Vinculin (1:2,000; 66305-1-Ig, Proteintech), Lamin A/C (1:1,000; 2032, Cell Signaling Technology), horseradish peroxidase-conjugated horse anti-mouse IgG (1:2,000; PI-2000, Vector Laboratories, Burlingame, CA, USA), and HRP-conjugated goat anti-rabbit IgG (1:2,000; 7074, Cell Signaling Technology).

*Fractionation of nuclear and cytoplasmic proteins*. GSCs were treated with JCI-20679 at the indicated concentrations for the indicated durations, and then cellular proteins were fractionated into nuclear and cytoplasmic fractions using a LysoPure nuclear and cytoplasmic extractor kit (295-73901, Wako) according to the manufacturer's protocol.

*Calcineurin activity assay*. The differentiated glioblastoma cells were treated with JCI-20679 at the indicated concentrations for 72 h. The cells were harvested, and calcineurin phosphatase activity in the same number of the cells was measured using a calcineurin cellular activity assay kit (BML-AK816, Enzo Life Sciences, Farmingdale, NY, USA) following the manufacturer's instructions. At least 10,000 cells per specimen were measured.

*Reverse transcription-quantitative PCR*. Cells were lysed with Trizol (15596026, Thermo Fisher Scientific) to extract total RNA. The RNAs were purified with an RNeasy mini kit (74106, Qiagen, Hilden, Germany). Quantitative PCR analysis was performed with THUNDERBIRD SYBR qPCR mix (QPS-201, TOYOBO, Osaka, Japan) using cDNA synthesized from the extracted RNAs using ReverTra Ace qPCR RT master mix with gDNA (genome DNA) remover (FSQ-301, TOYOBO) and a Light Cycler 96 system (Roche). A standard ΔCt method which had been reported previously (20) was used for data analysis. Gene expression levels were normalized to mGAPDH. Primers were obtained from Eurofins Genomics (Tokyo, Japan). The following primers were used: mNFATc2 primer #1 (F: GTGCAGCTCCACGGCTACAT, R: GCGGCT TAAGGATCCTCTCA), mNFATc2 primer #2 (F: GAGAAG ACTACAGATGGGCAG, R: ACTGGGTGGTAGGTAAAG TG), mGAPDH (F: GGTGTGAACGGATTTGGCCGTATT G, R: CCGTTGAATTTGCCGTGAGTGGAGT).

*NFATc2 overexpression*. NFATc2 overexpression was performed using a mouse neural stem-cell nucleofector kit (VPG-1004; Lonza, Tokyo, Japan) and a nucleofector 2b device (AAB-1001, Lonza) with an A-033 program optimized for mouse GSCs. The NFATc2 gene (MR209524, Origene Technology, Rockville, USA) or empty vector (PS100001, Origene) was introduced into mouse GSCs, and cells containing the NFATc2 gene or empty vector were selected using 50-250 μg/ml G418 (09380-86, Nacalai Tesque) for 2 weeks. The procedure was performed following the manufacturer's instructions. The nucleofection efficacy was confirmed by western blot analysis.

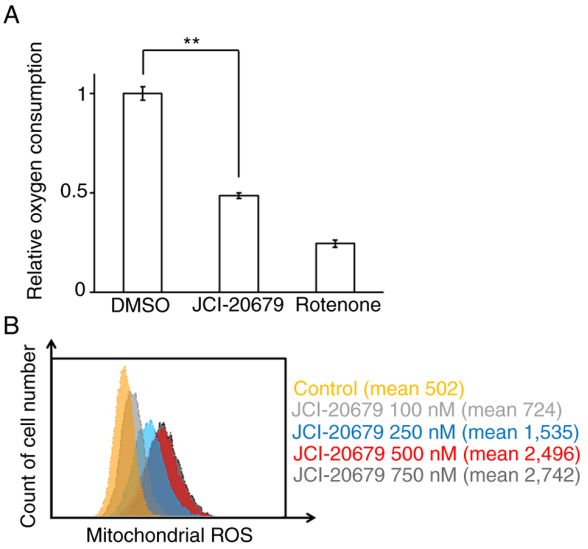


Figure 2. JCI-20679 inhibits mitochondrial functions. (A) Relative oxygen consumption in GSCs pretreated with 1 μM JCI-20679 or 1 μM rotenone as a positive control for 24 h (n=3). Data are presented as mean ± SD. $^{**}$P<0.01 by one-way ANOVA with Dunnett's multiple comparisons test. (B) Mitochondrial ROS generation in the differentiated glioblastoma cells treated with the indicated concentrations of JCI-20679. GSCs, glioblastoma stem-cells; ROS, reactive oxygen species; DMSO, dimethyl sulfoxide.

*Transplantation assay*. GSCs were injected into 20 sex-matched mice (6 weeks old; n=10 in each treatment group) for the analyzing the event-free survival rate, and GSCs of a deferent line were injected into 14 sex-matched mice (6 weeks old; n=7 in each treatment group) for the assessing the glioblastoma size. Cells ($1x10^3$) were suspended in 2 μl PBS (166-23555, Wako Pure Chemical Industries). Mice were anchored to the stereotaxic instrument. Cells were injected at a speed of 1 μl/min with an infusion system (Legato 130). The syringe was withdrawn from the brain 2 min after the injection. JCI-20679 was injected intraperitoneally at 20 mg/kg three times a week. JCI-20679 was dissolved at 10 mg/ml in DMSO with Kolliphor EL (C5135, Sigma-Aldrich) (final 10%) and then diluted in saline (total 200 μl/20 g body weight) to the required concentration. DMSO was used as a control. The occurrence of death, obvious neurological symptoms, or a decrease in body weight of more than 2 g was used to generate event-free survival curves. The JCI-20679 treatment was started after 3 days from the GSCs transplantation to analyze the event-free survival rate. Tumor formation was analyzed every week 10 min after injection of D-luciferin (126-05116, Wako) into the abdominal cavity of mice using an IVIS Lumina XR imaging system. For comparison of bioluminescence intensity, tumor initiation ($1x10^4$-$5x10^5$ photons/sec) was confirmed and then randomized before starting treatment. Mice with neurological symptoms by the tumor formation, such as slow moving or abnormal posture, were sacrificed by using cervical dislocation.

*Statistical analysis*. Two-tailed unpaired Student's t-test, two-tailed Welch's t-test, one-way ANOVA with Dunnett's

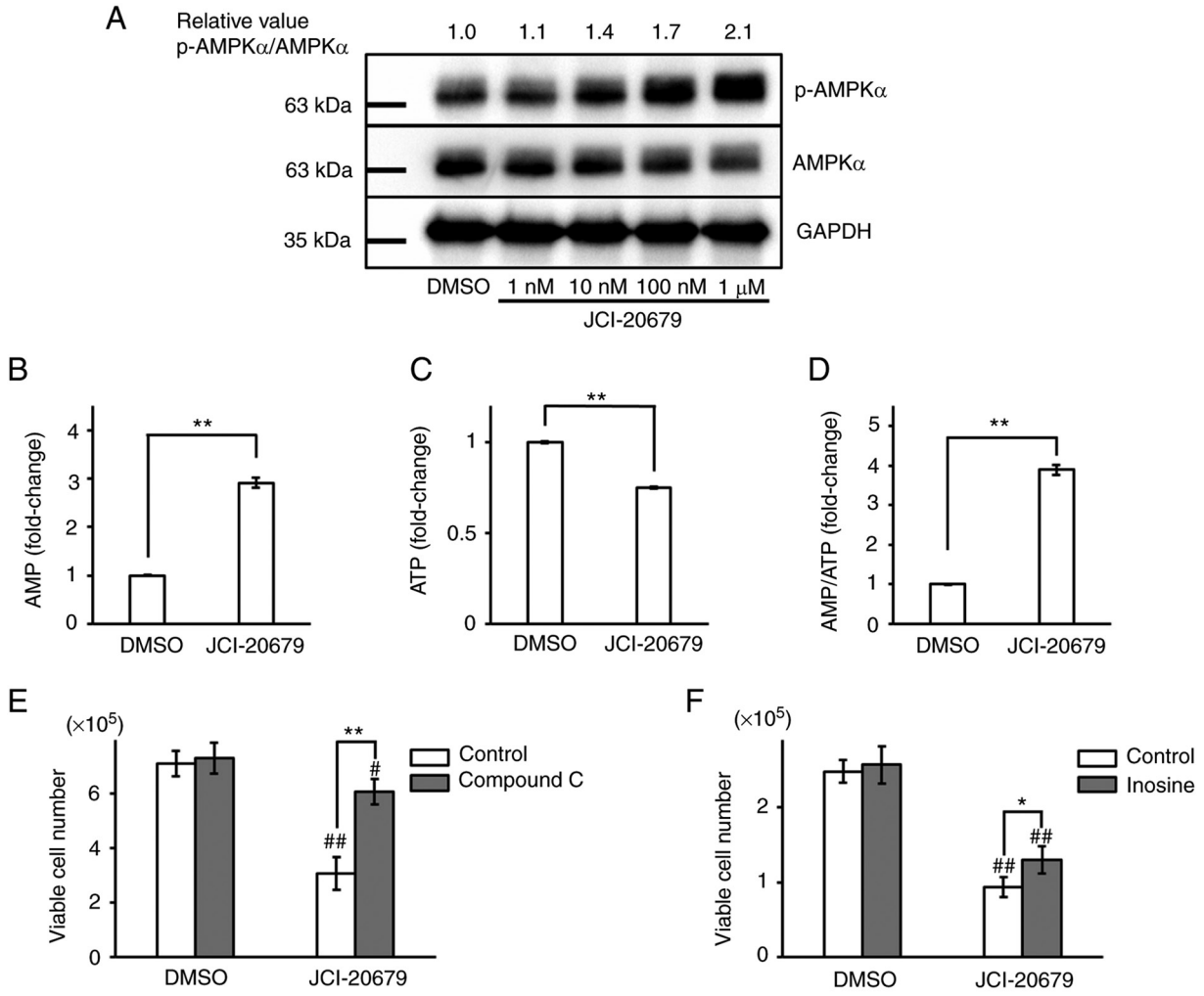


Figure 3. JCI-20679 activates AMPK. (A) Expression levels of p-AMPKα proteins in GSCs treated with JCI-20679 at the indicated concentrations for 24 h. Protein expression was evaluated using western blot analysis. Intracellular (B) AMP and (C) ATP levels in GSCs treated with 1 $\mu$M JCI-20679 for 24 h (n=4, respectively). (D) AMP/ATP ratio calculated from the measured AMP and ATP levels (n=4). (E) Viable cell numbers of GSCs treated with or without 50 nM JCI-20679 and with or without 75 nM compound C for 72 h (n=3). The number of viable cells was counted using trypan blue staining. (F) Viable cell numbers of U251 human glioblastoma cells treated with or without 500 nM JCI-20679 and with or without 500 $\mu$M inosine for 6 days (n=4). The number of viable cells were counted using trypan blue staining. $^{*}$P<0.05, $^{**}$P<0.01 as indicated; $^{\#}$P<0.05, $^{\#\#}$P<0.01 vs. DMSO by (B and D) two-tailed Welch's t-test, (C) two-tailed unpaired Student's t-test and (E and F) 2-way ANOVA with Bonferroni's multiple comparison test. All graphs represent mean ± SD. p-, phosphorylated; GSCs, glioblastoma stem cells; DMSO, dimethyl sulfoxide.

multiple comparison test or 2-way ANOVA with Bonferroni's multiple comparison test were used to determine the statistical significance for *in vitro* studies. Data are displayed as the mean ± SD unless otherwise indicated. All analyzed data were obtained from at least 3 independent experiments. For the *in vivo* study, log-rank tests were used to determine significant differences in the survival curves by the Kaplan-Meier method. Bioluminescence intensities were compared by Wilcoxon rank sum test. P-values were calculated using Microsoft Excel software. P<0.05 was considered statistically significant.

## Results

*JCI-20679 suppresses the proliferation of glioblastoma stem cells*. First, we analyzed the effects of JCI-20679 on the proliferation of GSCs maintained as neurospheres and differentiation-induced cells in adherent culture; both cell types were derived from identical murine glioblastoma tissues (Fig. 1A). The properties of GSCs and differentiation-induced cells have been established and described previously (17). We found that the proliferation of GSCs was more effectively suppressed by JCI-20679 than the proliferation of differentiated cells (Fig. 1B). JCI-20679 suppressed the proliferation of GSCs in a concentration-dependent manner (Fig. 1C). JCI-20679 treatment did not increase the number of trypan blue-positive dead cells (data not shown). In addition, the BrdU incorporation assay showed that JCI-20679 significantly reduced the number of cells entering the DNA synthesis phase of the cell cycle (Fig. 1D, E). However, we observed no significant induction of apoptosis by the Annexin-V assay and sub-G1 population by the cell cycle analysis (data not shown). These results suggest that JCI-20679 suppresses GSCs proliferation by inducing not apoptosis but cell cycle arrest.

*JCI-20679 inhibits mitochondrial function*. A previous study showed that JCI-20679 inhibits the function of the bovine mitochondria complex I *in vitro* (15). We next investigated the effects of JCI-20679 on mitochondrial function in cancer

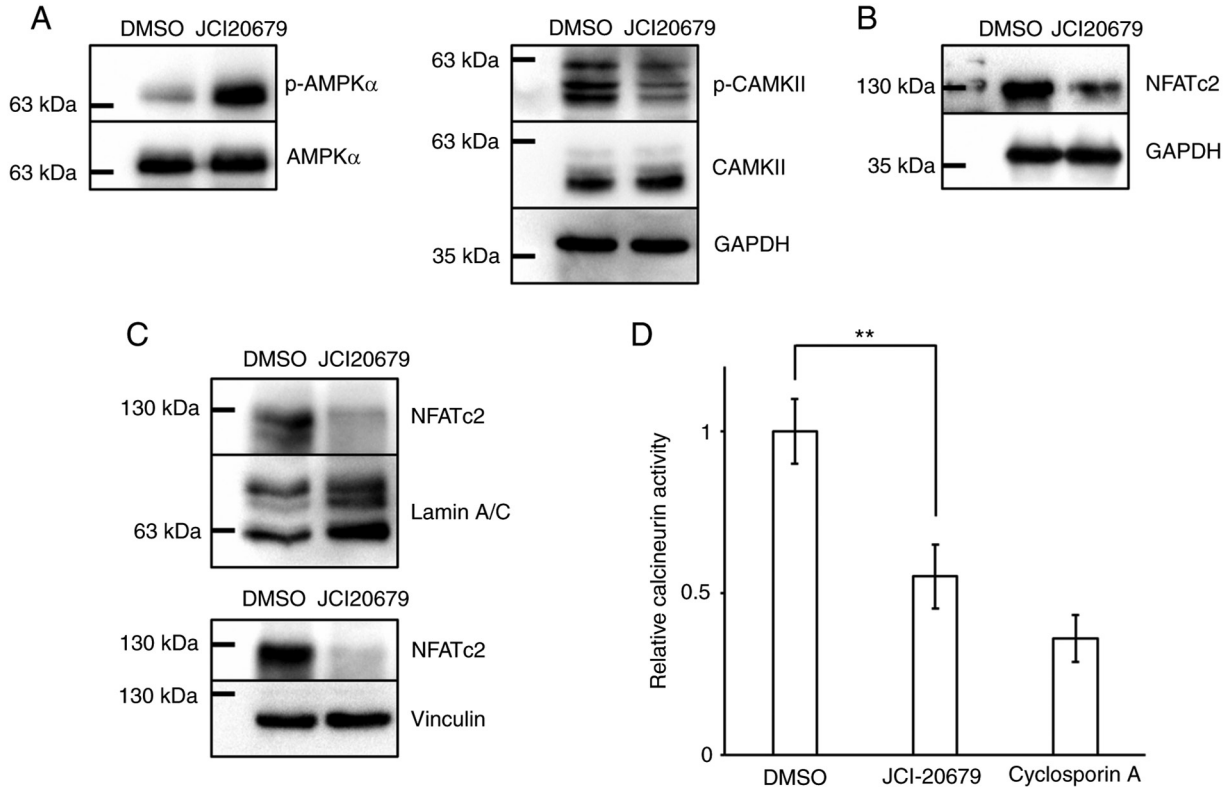


Figure 4. JCI-20679 reduces NFATc2 expression levels. (A) Expression levels of p-AMPKα and p-CAMKII proteins in GSCs treated with 100 nM JCI-20679 for 48 h. (B) Expression levels of NFATc2 proteins in GSCs treated with 500 nM JCI-20679 for 72 h. (C) Expression levels of NFATc2 proteins in the nucleus (upper panel) and cytoplasm (bottom panel) of GSCs treated with 500 nM JCI-20679 for 48 h. Protein levels were detected using western blot analysis. (D) Calcineurin phosphatase activity in the differentiated glioblastoma cells treated with 500 nM JCI-20679 or 10 $\mu$M cyclosporin A for 72 h (DMSO, n=12; JCI-20679, n=6; cyclosporin A, n=6). Data are presented as mean ± SD. $^{**}$P<0.01 by one-way ANOVA with Dunnett's multiple comparisons test. NFATc2, nuclear factor of activated T-cells 2; p-, phosphorylated; CAMKII, $Ca^{2+}$/calmodulin-dependent protein kinase II; GSCs, glioblastoma stem cells; DMSO, dimethyl sulfoxide.

cells. It was difficult to detect the mitochondrial membrane potential, which directly reflects mitochondrial function, in GSCs so we used the differentiated glioblastoma cells and A172 human glioblastoma cells as models. JCI-20679 significantly reduced the mitochondrial membrane potential, as did the established mitochondrial inhibitor CCCP, which was used as a positive control (Fig. S1A, B). We next measured the oxygen consumption rate of GSCs. JCI-20679 inhibited the oxygen consumption rate, which is an index of oxidative phosphorylation. Rotenone, an established mitochondrial complex I inhibitor, was used as a positive control (Fig. 2A). Moreover, we found that JCI-20679 increased mitochondrial ROS generation in the differentiated glioblastoma cells in a concentration-dependent manner (Fig. 2B). These results indicate that JCI-20679 inhibits mitochondrial function in cancer cells.

*JCI-20679 activates AMPK*. Inhibition of mitochondrial function activates AMPK through its phosphorylation (21), so we evaluated p-AMPKα protein levels in GSCs treated with JCI-20679. Our results showed that JCI-20679 concentration-dependently increased p-AMPKα protein levels (Fig. 3A). Consistent with these results, treatment of GSCs with JCI-20679 decreased intracellular ATP levels and increased intracellular AMP levels, resulting in a significant increase in the AMP/ATP ratio (Fig. 3B-D). Co-treatment with compound C or inosine, which are known AMPK inhibitors, significantly reversed the JCI-20679-mediated suppression of cell proliferation (Fig. 3E, F). These results suggest that JCI-20679 activates AMPK to suppress GSC proliferation.

*JCI-20679 reduces the expression of NFATc2*. Inhibition of mitochondrial function modulates the calcium signaling pathway (22), so we investigated the effect of JCI-20679 on factors involved in the calcium signaling pathway. Our results showed that JCI-20679 significantly reduced the protein levels of p-CaMKII and NFATc2 in GSCs (Fig. 4A, B). NFATc2 protein levels decreased in both nuclear and cytoplasmic protein fractions (Fig. 4C). Adequate quality of cellular fractionation was confirmed by western blot analysis (Fig. S1C). Moreover, JCI-20679 reduced calcineurin phosphatase activity (Fig. 4D). These results suggest that JCI-20679 suppresses the calcium signaling pathway.

*JCI-20679 suppresses the proliferation of glioblastoma stem cells by activating AMPK and reducing NFATc2 expression*. We next investigated the implication of the JCI-20679-mediated reduction in NFATc2 expression. JCI-20679 decreased NFATc2 mRNA levels in GSCs (Fig. 5A). It has been reported that AMPKα phosphorylation is suppressed by knockdown of AMPKβ, which is crucial for AMPKα phosphorylation (21). Thus, we used AMPKβ shRNA for suppressing AMPK

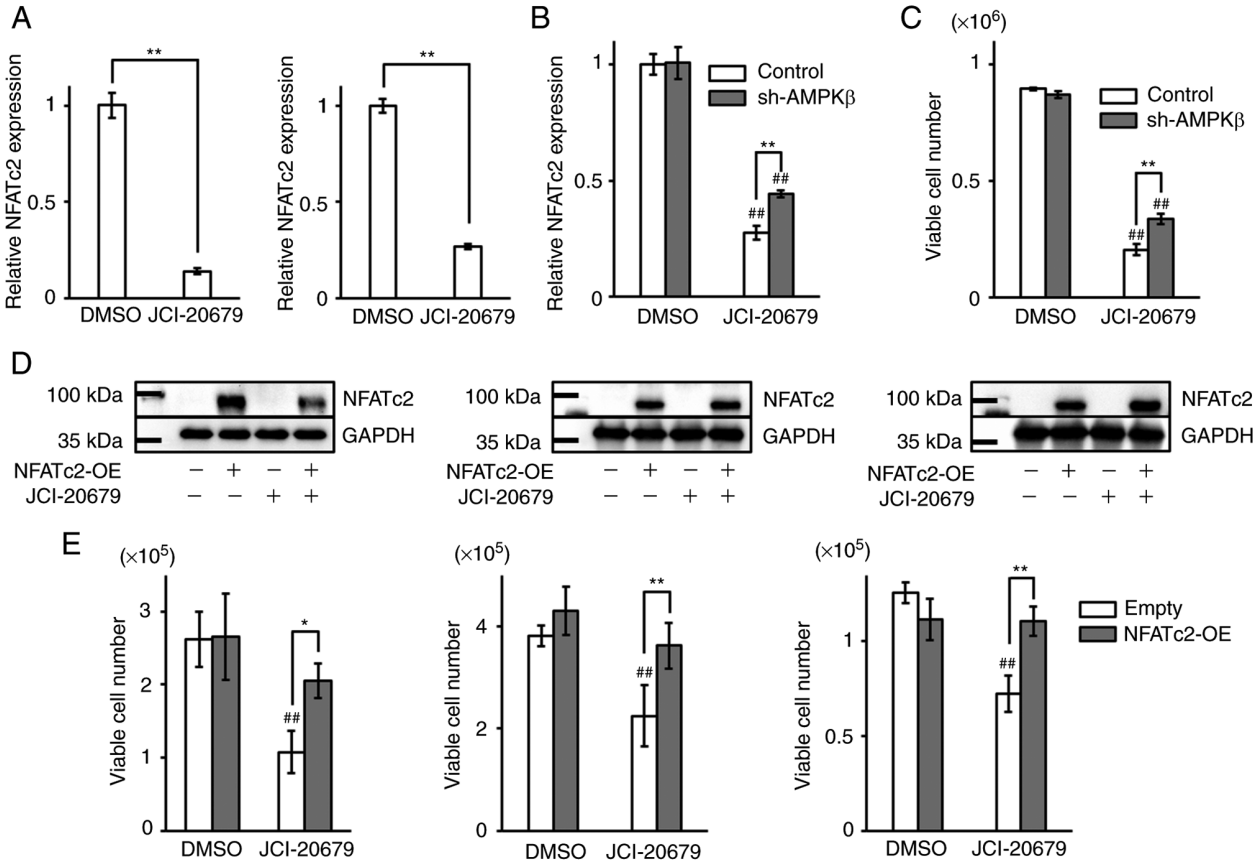


Figure 5. JCI-20679 suppresses the proliferation of GSCs by activating AMPK and decreasing NFATc2 expression. (A) NFATc2 mRNA levels in two different GSCs were treated with 1 $\mu$M JCI-20679 for 72 h. NFATc2 mRNA levels were analyzed using RT-qPCR (n=3 respectively). $^{**}$P<0.01 by two-tailed unpaired Student's t-test. (B) NFATc2 mRNA levels in AMPKβ-depleted (sh-AMPKβ) or control GSCs treated with 1 $\mu$M JCI-20679 for 24 h. NFATc2 mRNA levels were analyzed using RT-qPCR (n=3). $^{**}$P<0.01 as indicated; $^{\#\#}$P<0.01 vs. DMSO by 2-way ANOVA with Bonferroni's multiple comparison test. (C) Number of viable GSCs AMPKβ-depleted (sh-AMPKβ) or control after treatment with 100 nM JCI-20679 for 72 h (n=3). The number of viable cells were counted using trypan blue staining. $^{**}$P<0.01 as indicated, $^{\#\#}$P<0.01 vs. DMSO by 2-way ANOVA with Bonferroni's multiple comparison test. (D) NFATc2 expression was assessed using western blot analysis in GSCs (left and center panels) and differentiated glioblastoma cells (right panel) after treatment with JCI-20679 for 72 h. (E) Number of viable GSCs (left and center panels) and differentiated glioblastoma cells (right panel) after treatment with JCI-20679 for 72 h. Cells expressed either an empty vector (empty) or an NFTAc2 overexpression vector (NFATc2-OE) (n=3, respectively). The number of viable cells were counted using trypan blue staining. $^{*}$P<0.05, $^{**}$P<0.01 as indicated; $^{\#\#}$P<0.01 vs. DMSO by 2-way ANOVA with Bonferroni's multiple comparison test. Data are presented as mean ± SD. GSCs, glioblastoma stem cells; RT-qPCR, reverse transcription-quantitive PCR; NFATc2, nuclear factor of activated T-cells 2; sh-, short hairpin; -OE, -overexpression; DMSO, dimethyl sulfoxide.

activation. We confirmed suppressing AMPK activation successfully by western blot analysis. In addition, depleted AMPKβ has no effect on expression levels of NFATc2 protein (Fig. S1D). The decrease of NFATc2 mRNA levels mediated by JCI-20679 treatment was recovered when phosphorylation of AMPKα was suppressed (Fig. 5B). Furthermore, the experiment used another shRNA sequence and another NFATc2 primer gave similar result (Fig. S1E). In addition, cell viability of GSCs treated by JCI-20679 were recovered by knockdown of AMPKβ (Fig. 5C). Moreover, we tested the effects of NFATc2 overexpression in GSCs and differentiated glioblastoma cells. We confirmed NFATc2 overexpression by western blot analysis (Fig. 5D). NFATc2 overexpression significantly reversed the JCI-2067-mediated suppression of proliferation (Fig. 5E). These results indicate that the anti-proliferative effects of JCI-20679 are mediated by decreased NFATc2 expression levels that are caused by AMPK activation.

*JCI-20679 suppresses tumorigenicity in vivo*. To examine the antitumor effects of JCI-20679 *in vivo*, JCI-20679 was administered intraperitoneally (20 mg/kg three times a week) to a mouse model orthotopically transplanted with GSCs. JCI-20679 significantly improved event-free survival (Fig. 6A). We confirmed the efficacy of JCI-20679 using orthotopically transplanted with a different GSC line. JCI-20679 significantly decreased the luminescent signal, which reflects glioblastoma size, 3 weeks after JCI-20679 treatment was initiated (Fig. 6B, C). These results indicate that JCI-20679 suppresses glioblastoma proliferation *in vivo*.

## Discussion

In this study, we showed that JCI-20679 suppresses GSC proliferation by causing cell-cycle arrest. JCI-20679 decreased the mitochondrial membrane potential and suppressed the oxygen consumption rate, and increased the generation of mitochondrial ROS. These results are consistent with previous findings showing that JCI-20679 has inhibitory effects on mitochondrial function. AMPK is the molecule that senses the metabolic stress caused by inhibition of oxidative phosphorylation in

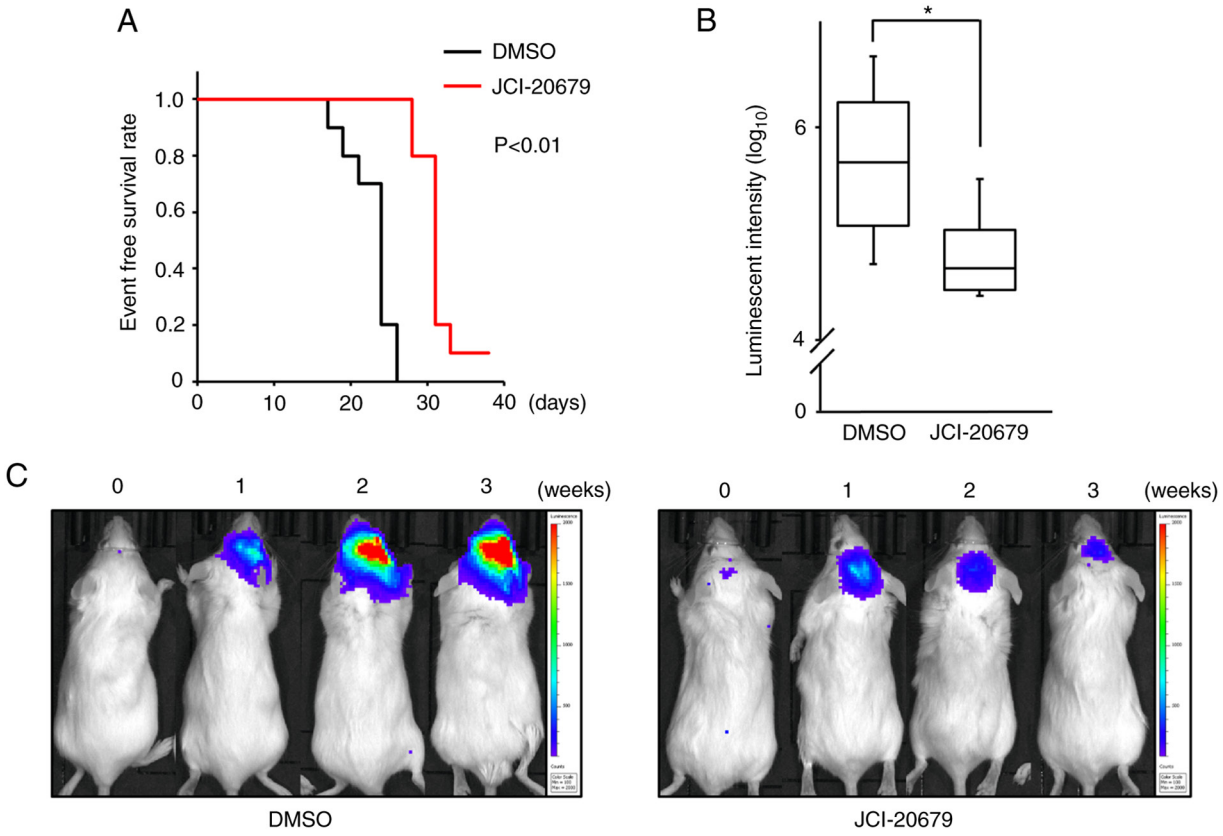


Figure 6. JCI-20679 extends overall event-free survival. (A) Event-free survival rate in mice orthotopically transplanted with GSCs intraperitoneally treated with either DMSO or JCI-20679 (20 mg/kg; n=10 in each treatment group). The event-free survival rate was analyzed using the Kaplan-Meier method. P<0.01 by log-rank tests. (B) Glioblastoma size assessed using bioluminescence intensity in mice orthotopically transplanted with a different GSC line and intraperitoneally treated with DMSO or JCI-20679 (20 mg/kg; n=7 for each treatment group). The luminescence values ($log_{10}$) after 3 weeks of treatment are shown. *P<0.05 by Wilcoxon rank sum test. (C) Representative images of the mice treated with DMSO or JCI-20679 are presented. GSCs, glioblastoma stem cells; DMSO, dimethyl sulfoxide.

mitochondria; an increase in the AMP/ATP ratio causes phosphorylation of AMPK (23). We found that JCI-20679 increased the AMP/ATP ratio and phosphorylated AMPK protein levels. AMPK inhibitors prevented JCI-206790-mediated suppression of GSC proliferation, suggesting that JCI-20679 suppresses GSCs proliferation by inhibiting mitochondrial functions, which activate AMPK.

We also found that JCI-20679 suppresses NFATc2 expression at the mRNA and protein levels; NFATc2 expression is regulated by calmodulin and calcineurin (24). Consistent with this finding, inhibition of mitochondrial complex I by knockdown of the GRIM-19 subunit suppresses NFATc2 expression and impairs heart development (25). Importantly, NFATc2 is highly expressed in glioblastoma tissue and is involved in cancer metastasis and invasion, and the calcineurin inhibitor cyclosporin A suppresses the growth of human glioblastoma cell lines (26). NFATc2 is more highly expressed in human GSCs than in differentiated glioblastoma cells (27). Moreover, an inhibitor of the calcineurin-NFAT pathway has anticancer effects in mice transplanted with glioblastoma cells (28). These findings suggest that NFATc2 is a promising molecular target for glioblastoma treatment. We found that JCI-20679 suppressed calcineurin activity, resulting in decreased NFATc2 expression levels. NFATc2 overexpression reversed the anti-proliferative effects of JCI-20679. These results indicate that the mechanism of action for JCI-20679 involves a decrease in NFATc2 expression.

Furthermore, we investigated the mechanisms underlying the JCI-20679-mediated suppression of NFATc2 expression. Inhibition of AMPKα recovered JCI-20679-mediated decreases in NFATc2 expression levels. It has been reported that activation of AMPK suppresses NFAT transcription by resveratrol treatment in a cardiac hypertrophy model (29). These results suggest that JCI-20679 inhibits mitochondrial function, which activates AMPK, leading to reduced NFATc2 expression levels. AMPK is also activated by the generation of mitochondrial ROS (30). Given that JCI-20679 induced mitochondrial ROS activity, AMPK may be activated by the generation of mitochondrial ROS in GSCs.

We showed that JCI-20679 inhibited the progression of glioblastoma *in vivo*. Mitochondrial inhibition is a promising novel therapeutic strategy for the treatment of cancer (31), including glioblastoma (32). Metformin, which inhibits oxidative phosphorylation in mitochondria, is being tested clinically in combination with temozolomide (33). In addition, AMPK activation is involved in the anticancer mechanisms of metformin (34). These findings support the notion that JCI-20679 may be an effective glioblastoma treatment *in vivo*.

Taken together, our results show that JCI-20679 inhibits mitochondrial function in cancer cells and exhibits

anti-proliferative effects in GSCs. We also show that JCI-20679 inhibits proliferation by activating AMPK and suppressing NFATc2 expression levels. Moreover, our *in vivo* studies show that JCI-20679 has potential as a new therapeutic agent against glioblastoma.

**Acknowledgements**

The authors would like to thank Ms. Satomi Toma, Ms. Shoko Inoie, Ms. Seiko Okamoto, Ms. Natsuko Tanaka and Mr. Hitoshi Iwasaki (Kyoto Pharmaceutical University, Kyoto, Japan) for experimental support.

**Funding**

This work was supported by the Japan Society for the Promotion of Science (grant nos. 16K08330, 20K07623 and 21K09167); the Ministry of Education, Culture, Sports, Science and Technology-Supported Program for the Strategic Research Foundation at Private Universities (grant no. S1511024L; between 2015 and 2019).

**Availability of data and materials**

The datasets used and/or analyzed during the current study are available from the corresponding author on reasonable request.

**Author's contributions**

SA, NK, CM, KO, HI and SN conducted experiments. SA, CM, HI and SN performed data analysis. NK, MF and SN participated in research design and supervised the study. SA and SN wrote the manuscript. SA, HI and SN confirmed the authenticity of all the raw data. All authors read and approved the final manuscript.

**Ethics approval and consent to participate**

All animal experiments were carried out under the approval of the Institutional Ethics Committee for Animal Experiments of Kyoto Pharmaceutical University (approval no. A21-001).

**Patient consent for publication**

Not applicable.

**Competing interests**

The authors declare that they have no competing interests.

**References**

1. Stupp R, Mason WP, van den Bent MJ, Weller M, Fisher B, Taphoorn MJ, Belanger K, Brandes AA, Marosi C, Bogdahn U, *et al*: Radiotherapy plus concomitant and adjuvant temozolomide for glioblastoma. N Engl J Med 352: 987-996, 2005.
2. Marenco-Hillembrand L, Wijesekera O, Suarez-Meade P, Mampre D, Jackson C, Peterson J, Trifiletti D, Hammack J, Ortiz K, Lesser E, *et al*: Trends in glioblastoma: Outcomes over time and type of intervention: A systematic evidence based analysis. J Neurooncol 147: 297-307, 2020.
3. Chinot OL, Wick W, Mason W, Henriksson R, Saran F, Nishikawa R, Carpentier AF, Hoang-Xuan K, Kavan P, Cernea D, *et al*: Bevacizumab plus radiotherapy-temozolomide for newly diagnosed glioblastoma. N Engl J Med 370: 709-722, 2014.
4. Sancho P, Barneda D and Heeschen C: Hallmarks of cancer stem cell metabolism. Br J Cancer 114: 1305-1312, 2016.
5. Singh SK, Hawkins C, Clarke ID, Squire JA, Bayani J, Hide T, Henkelman RM, Cusimano MD and Dirks PB: Identification of human brain tumour initiating cells. Nature 432: 396-401, 2004.
6. Schonberg DL, Lubelski D, Miller TE and Rich JN: Brain tumor stem cells: Molecular characteristics and their impact on therapy. Mol Aspects Med 39: 82-101, 2014.
7. Bueno MJ, Ruiz-Sepulveda JL and Quintela-Fandino M: Mitochondrial inhibition: A treatment strategy in cancer? Curr Oncol Rep 23: 49, 2021.
8. Yang SH, Li S, Lu G, Xue H, Kim DH, Zhu JJ and Liu Y: Metformin treatment reduces temozolomide resistance of glioblastoma cells. Oncotarget 7: 78787-78803, 2016.
9. Gao X, Yang Y, Wang J, Zhang L, Sun C, Wang Y, Zhang J, Dong H, Zhang H, Gao C, *et al*: Inhibition of mitochondria NADH-Ubiquinone oxidoreductase (complex I) sensitizes the radioresistant glioma U87MG cells to radiation. Biomed Pharmacother 129: 110460, 2020.
10. Myint SH, Cortes D, Laurens A, Hocquemiller R, Lebœuf M, Cavé A, Cotte J and Quéro AM: Solamin, a cytotoxic mono-tetrahydrofuranic γ-lactone acetogenin from Annona muricata seeds. Phytochemistry 30: 3335-3338, 1991.
11. Kojima N, Fushimi T, Tatsukawa T, Tanaka T, Okamura M, Akatsuka A, Yamori T, Dan S, Iwasaki H and Yamashita M: Thiophene-3-carboxamide analogue of annonaceous acetogenins as antitumor drug lead. Eur J Med Chem 86: 684-689, 2014.
12. Ohta K, Akatsuka A, Dan S, Iwasaki H, Yamashita M and Kojima N: Structure-activity relationships of thiophene carboxamide annonaceous acetogenin analogs: Shortening the alkyl chain in the tail part significantly affects their growth inhibitory activity against human cancer cell lines. Chem Pharm Bull (Tokyo) 69: 1029-1033, 2021.
13. Matsumoto T, Akatsuka A, Dan S, Iwasaki H, Yamashita M and Kojima N: Synthesis and cancer cell growth inhibition effects of acetogenin analogs bearing ethylene glycol units for enhancing the water solubility. Tetrahedron 76: 131058, 2020.
14. Matsumoto T, Kojima N, Akatsuka A, Yamori T, Dan S, Iwasaki H and Yamashita M: Convergent synthesis of stereoisomers of THF ring moiety of acetogenin thiophene analogue and their antiproliferative activities against human cancer cell lines. Tetrahedron 73: 2359-2366, 2017.
15. Akatsuka A, Kojima N, Okamura M, Dan S and Yamori T: A novel thiophene-3-carboxamide analog of annonaceous acetogenin exhibits antitumor activity via inhibition of mitochondrial complex I. Pharmacol Res Perspect 4: e00246, 2016.
16. Wiesner SM, Decker SA, Larson JD, Ericson K, Forster C, Gallardo JL, Long C, Demorest ZL, Zamora EA, Low WC, *et al*: De novo induction of genetically engineered brain tumors in mice using plasmid DNA. Cancer Res 69: 431-439, 2009.
17. Tanigawa S, Fujita M, Moyama C, Ando S, Ii H, Kojima Y, Fujishita T, Aoki M, Takeuchi H, Yamanaka T, *et al*: Inhibition of Gli2 suppresses tumorigenicity in glioblastoma stem cells derived from a de novo murine brain cancer model. Cancer Gene Ther 28: 1339-1352, 2021.
18. Fujita M, Scheurer ME, Decker SA, McDonald HA, Kohanbash G, Kastenhuber ER, Kato H, Bondy ML, Ohlfest JR and Okada H: Role of type 1 IFNs in antiglioma immunosurveillance-using mouse studies to guide examination of novel prognostic markers in humans. Clin Cancer Res 16: 3409-3419, 2010.
19. Taniguchi K, Kageyama S, Moyama C, Ando S, Ii H, Ashihara E, Horinaka M, Sakai T, Kubota S, Kawauchi A and Nakata S: γ-Glutamylcyclotransferase, a novel regulator of HIF-1α expression, triggers aerobic glycolysis. Cancer Gene Ther 29: 37-48, 2021.
20. Livak KJ and Schmittgen TD: Analysis of relative gene expression data using real-time quantitative PCR and the 2(-Delta Delta C(T)) method. Methods 25: 402-408, 2001.
21. Garcia D and Shaw RJ: AMPK: Mechanisms of cellular energy sensing and restoration of metabolic balance. Mol Cell 66: 789-800, 2017.
22. Pathak T and Trebak M: Mitochondrial Ca2+ signaling. Pharmacol Ther 192: 112-123, 2018.
23. Hardie DG, Ross FA and Hawley SA: AMPK: A nutrient and energy sensor that maintains energy homeostasis. Nat Rev Mol Cell Biol 13: 251-262, 2012.

24. Mognol GP, Carneiro FR, Robbs BK, Faget DV and Viola JP: Cell cycle and apoptosis regulation by NFAT transcription factors: New roles for an old player. Cell Death Dis 7: e2199, 2016.
25. Chen Y, Yuen WH, Fu J, Huang G, Melendez AJ, Ibrahim FB, Lu H and Cao X: The mitochondrial respiratory chain controls intracellular calcium signaling and NFAT activity essential for heart formation in Xenopus laevis. Mol Cell Biol 27: 6420-6432, 2007.
26. Tie X, Han S, Meng L, Wang Y and Wu A: NFAT1 is highly expressed in, and regulates the invasion of, glioblastoma multiforme cells. PLoS One 8: e66008, 2013.
27. Jiang Y, Song Y, Wang R, Hu T, Zhang D, Wang Z, Tie X, Wang M and Han S: NFAT1-mediated regulation of NDEL1 promotes growth and invasion of glioma stem-like cells. Cancer Res 79: 2593-2603, 2019.
28. Liu Z, Li H, He L, Xiang Y, Tian C, Li C, Tan P, Jing J, Tian Y, Du L, *et al*: Discovery of small-molecule inhibitors of the HSP90-calcineurin-NFAT pathway against glioblastoma. cell Chem Biol 26: 352-365.e7, 2019.
29. Chan AY, Dolinsky VW, Soltys CL, Viollet B, Baksh S, Light PE and Dyck JR: Resveratrol inhibits cardiac hypertrophy via AMP-activated protein kinase and Akt. J Biol Chem 283: 24194-201, 2008.
30. Rabinovitch RC, Samborska B, Faubert B, Ma EH, Gravel SP, Andrzejewski S, Raissi TC, Pause A, St-Pierre J and Jones RG: AMPK maintains cellular metabolic homeostasis through regulation of mitochondrial reactive oxygen species. Cell Rep 21: 1-9, 2017.
31. Ghosh P, Vidal C, Dey S and Zhang L: Mitochondria targeting as an effective strategy for cancer therapy. Int J Mol Sci 21: 3363, 2020.
32. Guntuku L, Naidu VG and Yerra VG: Mitochondrial dysfunction in gliomas: pharmacotherapeutic potential of natural compounds. Curr Neuropharmacol 14: 567-583, 2016.
33. Maraka S, Groves MD, Mammoser AG, Melguizo-Gavilanes I, Conrad CA, Tremont-Lukats IW, Loghin ME, O'Brien BJ, Puduvalli VK, Sulman EP, *et al*: Phase 1 lead-in to a phase 2 factorial study of temozolomide plus memantine, mefloquine, and metformin as postradiation adjuvant therapy for newly diagnosed glioblastoma. Cancer 125: 424-433, 2019.
34. Zhao B, Luo J, Yu T, Zhou L, Lv H and Shang P: Anticancer mechanisms of metformin: A review of the current evidence. Life Sci 254: 117717, 2020.